6788–6803 *Nucleic Acids Research, 2021, Vol. 49, No. 12* *Published online 16 June 2021*
https://doi.org/10.1093/nar/gkab489

Prostate cancer-associated SPOP mutations lead to genomic instability through disruption of the SPOP–HIPK2 axis

Xiaofeng Jin [1,3,*,†], Shi Qing [7,†], Qian Li [1,3], Hui Zhuang [1,3], Liliang Shen [4], Jinhui Li [1], Honggang Qi [5], Ting Lin [1,3], Zihan Lin [1,3], Jian Wang [1,3], Xinyi Cao [1,3], Jianye Yang [1,3], Qi Ma [6], Linghua Cong [4], Yang Xi [3], Shuai Fang [3], Xiaodan Meng [3], Zhaohui Gong [3], Meng Ye [1,3], Shuyun Wang [8,*], Chenji Wang [7,*] and Kun Gao [2,*]

[1]The Affiliated Hospital of Medical School, Ningbo University, Ningbo 315020, China, [2]Department of Clinical Laboratory, Shanghai First Maternity and Infant Hospital, Tongji University School of Medicine, Shanghai 201204, China, [3]Department of Biochemistry and Molecular Biology, Zhejiang Key Laboratory of Pathophysiology, Medical School of Ningbo University, Ningbo 315211, China, [4]Department of Urology, Department of Hematology, the Affiliated Yinzhou Renmin Hospital of Medical School of Ningbo University, Ningbo 315040, China, [5]Department of Urology, the Affiliated Yinzhou Second Hospital of Medical School of Ningbo University, Ningbo 315100, China, [6]Translational Research Laboratory for Urology, the Key Laboratory of Ningbo City. Ningbo First Hospital, The affiliated hospital of Ningbo University, Ningbo, Zhejiang 315010, China, [7]State Key Lab of Genetic Engineering, MOE Engineering Research Center of Gene Technology, School of Life Sciences, Fudan University, Shanghai 200438, China and [8]Department of Breast Surgery, Shanghai First Maternity and Infant Hospital, Tongji University School of Medicine, Shanghai 201204, China

Received July 24, 2020; Revised May 13, 2021; Editorial Decision May 15, 2021; Accepted May 20, 2021

ABSTRACT

Speckle-type Poz protein (SPOP), an E3 ubiquitin ligase adaptor, is the most frequently mutated gene in prostate cancer. The SPOP-mutated subtype of prostate cancer shows high genomic instability, but the underlying mechanisms causing this phenotype are still largely unknown. Here, we report that upon DNA damage, SPOP is phosphorylated at Ser119 by the ATM serine/threonine kinase, which potentiates the binding of SPOP to homeodomain-interacting protein kinase 2 (HIPK2), resulting in a nondegradative ubiquitination of HIPK2. This modification subsequently increases the phosphorylation activity of HIPK2 toward HP1γ, and then promotes the dissociation of HP1γ from trimethylated (Lys9) histone H3 (H3K9me3) to initiate DNA damage repair. Moreover, the effect of SPOP on the HIPK2-HP1γ axis is abrogated by prostate cancer-associated SPOP mutations. Our findings provide new insights into the molecular mechanism of SPOP mutations-driven genomic instability in prostate cancer.

INTRODUCTION

Large-scale whole-exome and whole-genome sequencing studies have revealed that recurrent mutations in the Speckle-type Poz protein (*SPOP*) gene occur in up to 15% of prostate cancers (1–3). A study performed in The Cancer Genome Atlas (TCGA) of prostate cancers showed that those harboring SPOP mutations have several notable molecular features, including mutual exclusivity of ETS rearrangement, elevated DNA methylation levels, and co-occurring CHD1 deletions, supporting the notion that SPOP-derived mutant tumors represent a distinct subclass of prostate cancer (2). SPOP is a substrate-binding adaptor of Cullin 3 (CRL3) E3 ubiquitin ligase complex (4). The majority of prostate cancer-associated SPOP mutations occur in the substrate-binding MATH domain, suggesting that these mutations may alter the interaction between SPOP and its substrates (1,2). We and others have identified multiple oncoproteins, such as SRC-3 (5), AR (6,7), ERG (8,9), DEK (10), BRD2/3/4 (11–13), PD-L1 (14), SENP7 (15),

*To whom correspondence should be addressed. Tel: +86 021 20261000; Email: kungao@tongji.edu.cn
Correspondence may also be addressed to Xiaofeng Jin. Tel: +86 0574 87609951; Email: jinxiaofeng@nbu.edu.cn
Correspondence may also be addressed to Chenji Wang. Email: chenjiwang@fudan.edu.cn
Correspondence may also be addressed to Shuyun Wang. Email:2000672@tongji.edu.cn
†The authors wish it to be known that, in their opinion, the first two authors should be regarded as Joint First Authors.

c-MYC (16), Cyclin E1 (17) and Nanog (18,19), that are ubiquitinated and degraded by the CRL3–SPOP ubiquitin ligase complex. Moreover, CRL3–SPOP ubiquitin ligase complex may exert its tumor-suppressive function by regulating the non-degradative ubiquitination of INF2 (20) and MyD88 (21). Prostate cancer-associated SPOP mutations lead to an aberrant regulation of multiple oncogenic substrates, thereby promoting malignant phenotypes including enhanced cell proliferation and invasiveness, immune escape, and anticancer agent resistance.

Genomic instability resulting from DNA damage events caused by extrinsic agents or metabolic by-products is a main driving force towards tumorigenesis and cancer progression (22,23). To cope with the resulting genotoxicity, cells must detect DNA breaks and either transiently delay cell cycle progression to allow for time to repair the DNA lesion, and induce programmed cell death if the damage is too severe (22,23). Whole genome sequencing revealed that SPOP-mutated prostate cancer specimens displayed significantly higher number of genomic rearrangements. Mechanistically, SPOP mutations led to homology-directed repair (HR) defects, but promoting error-prone nonhomologous-mediated end joining (NHEJ) in cells. Given this effect, a synthetic lethality approach based on PARP inhibitors may represent a new strategy for treating SPOP-mutated prostate cancer (24). Another report suggested that SPOP may prevent replication stress and aberrant cell cycle progression by promoting the mRNA expression of DNA repair and replication factors, such as RAD51, BRCA2, CHEK1 and ATR (25). Nevertheless, little is known about which proteins are the direct downstream molecular mediators towards SPOP-mediated DNA damage response (DDR).

Homeodomain-interacting protein kinase 2 (HIPK2) is a serine/threonine protein kinase that is involved in multiple pathological conditions, and is known to play a diverse role in cell growth, senescence, differentiation, apoptosis, and development (26,27). HIPK2 senses various environmental stresses, and relays these signals into substrate phosphorylation effects, which in turn contributes towards cell survival or death (28). Previous studies have suggested that HIPK2 may play a dual effect on cell fate choice upon DNA damage, and these depend on the type and severity of cellular stress. For example, upon sublethal DNA damage, HIPK2 can stimulate DDR through phosphorylation of the epigenetic regulator HP1γ (29). Alternatively, in cases of non-repairable DNA damage, it can irreversibly drive cells to p53-dependent apoptosis by phosphorylating p53 at Ser46 (30–32). Although progress has been made in understanding the molecular mechanisms driving HIPK2-mediated DDR, specific signaling pathways involved remain largely unknown.

In this study, we reveal that upon DNA damage, SPOP functions as a positive regulator of DDR by binding to and inducing the non-degradative ubiquitination of HIPK2, which triggers the phosphorylation of HP1γ to promote DDR. However, these effects are abrogated by prostate cancer-associated SPOP mutations. Our findings suggest that SPOP-mediated HIPK2 ubiquitination is important for efficient DDR and towards maintaining genomic stability.

MATERIALS AND METHODS

Antibody, chemicals, primers and shRNA/sgRNA sequence information used in this study are listed in SI Appemdix, Supplementary Tables S1–S4.

Cell culture and reagents

293T and prostate cancer cell lines (PC-3 and DU145) were purchased from American Type Culture Collection. 293T cells were cultured in Dulbecco's modified Eagle's medium (DMEM) supplemented with 10% FBS. PC-3 and DU145 cells were cultured in RPMI 1640 medium supplemented with 10% FBS. The antibodies and chemicals used in this study are listed in Supplementary Tables S1 and S2.

Plasmid constructions

Expression vectors for SPOP were described previously (6). SPOP or HIPK2 mutants were generated by using a KOD-Plus-Mutagenesis Kit (TOYOBO) by following the manufacturer's instructions. The sequences of primers are listed in Supplementary Table S3.

Western blot

Cell lysates or immunoprecipitates were subjected to SDS–PAGE, and proteins were transferred to nitrocellulose membranes (GE Healthcare Sciences). Membranes were blocked in Tris-buffered saline (TBS, pH7.4) containing 5% non-fat milk and 0.1% Tween-20, washed twice in TBS containing 0.1% Tween-20 and incubated with primary antibody overnight at 4°C followed by secondary antibody for 1 h at room temperature. Proteins of interest were visualized using the Enhanced Chemiluminescence (ECL) system (Santa Cruz Biotechnology). WB was performed for 2–3 times from at least two independent experiments and representative pictures were shown.

GST pull-down assays

GST fusion proteins were immobilized on glutathione-Sepharose beads (Amersham Biosciences). After washing with pull-down buffer (20 mM Tris–HCl, pH 7.5, 150 mM NaCl, 0.1% NP-40, 1 mM DTT, 10% glycerol, 1 mM EDTA, 2.5 mM $MgCl_2$ and 1 μg/ml leupeptin), the beads were incubated with recombinant His-tagged protein for 2 h. The beads were then washed 5 times with binding buffer and resuspended in sample buffer. The bound proteins were subjected to SDS–PAGE and Western blot analysis.

In vivo ubiquitination assays

293T cells were transfected with HA–ubiquitin and the indicated constructs. Thirty-six hours after transfection, cells were treated with 30 μM MG132 for 6 h and then lysed in 1% SDS buffer (Tris [pH 7.5], 0.5 mM EDTA, 1 mM DTT) and boiled for 10 min. For immunoprecipitation, the cell lysates were diluted 10-fold in Tris–HCl buffer and incubated with anti-FLAG M2 agarose beads (Sigma) for 4 h at 4°C. The bound beads are then washed four times with BC100 buffer (20 mM Tris–Cl, pH 7.9, 100 mM NaCl, 0.2

mM EDTA, 20% glycerol) containing 0.2% Triton X-100. The protein was eluted with 3× FLAG peptide for 2 h at 4°C. The ubiquitinated form of HIPK2 was detected by Western blot using anti-HA antibody.

In vitro ubiquitination assays

In vitro ubiquitination assays were carried out using a protocol reported previously (10). Briefly, 2 μg of APP-BP1/Uba3, 2 μg of His-UBE2M enzymes and 5 μg of NEDD8 were incubated at 30°C for 2 h in the presence of ATP. The thioester-loaded His-UBE2M–NEDD8 was further incubated with 3 μg of His-DCNL2 and 6 μg of CUL3–RBX1 at 4°C for 2 h to obtain neddylated CUL3–RBX1. The neddylated CUL3–RBX1, 5 μg of GST-SPOP, 5 μg of ubiquitin, 500 ng of E1 enzyme, 750 ng of E2 enzyme (UbcH5a and UbcH5b) and 5 μg of GST-HIPK2 (purchased from Carna Bioscience) were incubated with 0.6 μl of 100 mM ATP, 1.5 μl of 20 μM ubiquitin aldehyde, 3 μl of 10× ubiquitin reaction buffer (500 mM Tris–HCl (pH 7.5), 50 mM KCl, 50 mM NaF, 50 mM $MgCl_2$ and 5 mM DTT), 3 μl of 10× energy regeneration mix (200 mM creatine phosphate and 2 μg/μl creatine phosphokinase) and 3 μl of 10× protease inhibitor cocktail at 30°C for 2 h, followed by western blot analysis. Ubiquitin, E1, E2 and CUL3–RBX1 were purchased from Ubiquigent.

In vitro kinase assays

GST–HIPK2-5KR in the pGEX-4T-2 vector was purified from *Escherichia coli* using glutathione–agarose (Sigma). GST–HIPK2-WT was purchased from Carna Bioscience. $(His)_6$–p53 in PET28a vector was purified from E. coli using a Ni-NTA minicolumn (Qiagen). $(His)_6$–p53 and recombinant kinases were incubated in a kinase buffer containing 50 mM Tris–HCl pH 7.5, 10 mM manganese chloride and 100 mM unlabeled ATP. After incubation for 30 min at 30°C, the reactions were terminated by addition of SDS sample buffer, and the reaction samples were separated by SDS-PAGE, followed by western blot analysis.

Proximity ligation assays

DU145 cells were seeded into 24-well chamber slides. After 24 h in DMEM, the cells were transfected with FLAG-HIPK2 and HA-SPOP plasmids. Twenty-four hours after transfection, cells were treated with ETO (75 μg/ml) or DMSO for 4 h, and then fixed with 4% paraformaldehyde. Cells were then permeabilized in 0.4% Triton X-100 and blocked in Duolink Blocking buffer (Sigma) for 1 h at 37°C. For the in situ PLA, we used the Duolink in situ Red kit (Sigma-Aldrich, DUO92101). Primary antibodies with anti-FLAG and anti-Myc were incubated overnight at 4°C. The next day, Plus and Mines PLA probes were incubated for 1 h at 37°C. Ligation and amplification of the PLA were performed using the Duolink In Situ Detection Reagents Red (Sigma). After several washes, cells were mounted in Prolong Gold mounting media with DAPI. Cells were imaged using a confocal microscope (LSM880, Zeiss) with a 63×/1.4NA Oil PSF Objective.

Mass spectrometry analysis of ubiquitin attachment sites

Ubiquitinated HIPK2 was prepared by transfecting FLAG–HIPK2, HA–Ub and Myc–SPOP into 293T cells and liquid chromatography–tandem mass spectrometry (LC–MS/MS) analysis was carried out at the proteomics center of our institute.

CRISPR-Cas9-mediated gene knock-out cell generation

The pX459 plasmid was used to clone guide oligos targeting the *SPOP* or *HIPK2* gene. Knock-out cell clones were screened through western blot analysis and validated via Sanger sequencing. The sequences of the gene-specific sgRNAs are listed in Supplementary Table S4.

Cell proliferation assays

Cell proliferation rate was determined by using Cell Counting Kit-8 (CCK-8) kit (Dojindo) in accordance with the manufacturer's protocol.

Cell death assays

The cells were stained with propidium iodide, and subjected to flow cytometry. The results were given as the representatives of three independent experiments with triplicate samples for each condition.

Colony formation assays

PC-3 or DU145 cells were seeded in six-well plates containing 1×10^3 individual cells per well in triplicate. After 2 weeks of incubation, the cell lines were fixed with 100% methanol for 5 min and then stained with Giemsa dye for 20 min.

Generation of xenograft mouse models

All experimental protocols were approved in advance by the Ethics Review Committee for Animal Experimentation of Ningbo University. 4–6-week-old BALB/c nu/nu mice obtained from SLAC Laboratory Animal Co., Ltd. were bred and maintained in our institutional pathogen-free mouse facilities. 5×10^6 PC-3 or DU145 cells were suspended in 100 μl of PBS buffer and injected into the flanks of male nude mice. At the end of 3 weeks, mice were killed and *in vivo* solid tumors were dissected and weighed.

Immunofluorescence and confocal microscopy

For immunofluorescence (IF) analysis, the cells were visualized and imaged by using a confocal microscope. Analytical results were obtained in triplicate from three different fields.

Comet assays

The Comet assays were as performed as previously described (33,34). Finally, the slides were examined, in a blind study, at 400× magnification with a Nikon Ti2 fluorescence microscope equipped with a 480–550-nm wide-band excitation filter and a 590-nm barrier filter, and images of cells

were analyzed with the Komet 3.1 Image Analysis System (Kinetic Imaging). Forty cells from each of the two replicate slides were analyzed per sample. A metric based on the concept of Olive tail moment (33). was computed utilizing the Komet software and used as measure of DNA damage.

Statistical analysis

All data are shown as mean values ± SD for experiments performed with at least three replicates. Statistical analyses were performed using the paired Student's *t*-test. * indicates $P < 0.05$; ** indicates $P < 0.01$; *** indicates $P < 0.001$.

RESULTS

Identification of HIPK2 as a novel SPOP interacting protein

Previously, we used FLAG-SPOP as bait to identify potential SPOP substrates via affinity-purification followed by mass spectrometry (AP-MS). From this experiment, HIPK2 ranked high on the interaction hit list (35). Given that HIPK2 participates in the regulation of diverse cellular activities, we decided to further identify whether SPOP exerts its tumor-suppressive roles partly through its interaction with HIPK2.

We first verified the binding of HIPK2 by SPOP via a coimmunoprecipitation (co-IP) assay. Ectopically expressed Myc–SPOP protein was coimmunoprecipitated by FLAG–HIPK2; conversely, Myc–HIPK2 protein was coimmunoprecipitated by FLAG–SPOP (Figure 1A, B). FLAG–SPOP was capable of immunoprecipitating endogenous HIPK2 and two known SPOP substrates, INF2 and BRD4, in PC-3 prostate cancer cells (Figure 1C). Importantly, endogenous SPOP–HIPK2 complex was present in PC-3 cells as demonstrated by co-IP with an SPOP antibody (Figure 1D). To determine whether the interaction between SPOP and HIPK2 is direct, we detected their interaction *in vitro* using purified recombinant proteins. As shown in Figure 1E, the GST pull-down assays showed that GST-HIPK2, but not the GST alone, bound to $(His)_6$-SPOP, suggesting that SPOP and HIPK2 physically interact with each other *in vitro*. Co-IP assays indicated that SPOP did not interact with HIPK1, which is a paralogous HIPK protein family member (Figure 1F). Only SPOP, and none of the other CUL3-based BTB domain-containing adaptors that we examined, interacted with HIPK2 (Figure 1G). The MATH domain of SPOP is responsible for recruiting substrates (4). In accordance with this notion, we demonstrated that the deletion of the MATH domain, but not that of the CUL3-binding BTB domain, totally abolished SPOP's capacity to interact with HIPK2 (Figure 1H, I). Immunofluorescence (IF) analysis showed that HIPK2 was colocalized with SPOP in the form of nuclear puncta in cells (Supplementary Figure S1A). Taken together, our findings suggest that SPOP specifically interacts with HIPK2 *in vivo* and *vitro*.

SPOP promotes HIPK2 ubiquitination but not degradation

We next explored whether SPOP promotes the ubiquitination and degradation of HIPK2. The ectopic expression of wild-type SPOP or its deletion mutants did not alter the protein levels of coexpressed HIPK2 (Figure 2A). Furthermore, stable overexpression of SPOP in two prostate cell lines (PC-3 and DU145) did not alter the protein levels of endogenous HIPK2 (Figure 2B). SPOP depletion via short hairpin RNA (shRNA)-mediated knockdown or CRISPR/Cas9-mediated knockout in PC-3 and DU145 cells did not alter HIPK2 protein levels (Figure 2C; Supplementary Figures S2, S3, S4A). To confirm loss of SPOP activity, BRD4, a known SPOP-degradative substrate, was stabilized in protein levels (Figure 2C; Supplementary Figure S4A). HIPK2 was robustly polyubiquitinated in a dose-dependent manner by SPOP–WT coexpression, but not by the SPOP–ΔBTB or SPOP–ΔMATH mutant (Figure 2D). Accordingly, a depletion of SPOP decreased the endogenous ubiquitination of HIPK2 (Supplementary Figure S4B). We further demonstrated that the SPOP–CUL3–RBX1 complex catalyzed HIPK2 ubiquitination *in vitro* (Figure 2E).

Given that SPOP-mediated HIPK2 ubiquitination was non-degradative, we then examined the linkage specificity of SPOP-mediated HIPK2 ubiquitination. We performed an *in vivo* ubiquitination assay by using a panel of ubiquitin mutants containing a single K→R mutation at each of the seven lysines in ubiquitin that may be involved in the formation of polyubiquitin chains. We also included a lysine-free ubiquitin mutant wherein all the lysines were replaced with arginines (K-ALL-R). The expression of the Ub (K-ALL-R) mutant abolished SPOP-mediated HIPK2 ubiquitination, excluding the possibility that SPOP promoted multiple mono-ubiquitination events on HIPK2 (Figure 2F). The expression of Ub-K6R or K11R did not alter the amount of ubiquitinated HIPK2 (Figure 2G), suggesting that Ub-K6, and K11 were largely dispensable for SPOP-mediated HIPK2 ubiquitination. By contrast, a moderate reduction in HIPK2 ubiquitination was observed when using Ub-K27R, K29R, K33R, K48R and K63R (Figure 2G). We then chose to use a reciprocal series of mutants. These mutants contained only one lysine, with the other six lysines mutated to arginines. As shown in Figure 2F, the expression of K27O, K29O, K33O, K48O or K63O Ub mutants markedly abolished SPOP-mediated HIPK2 ubiquitination. These data suggest that SPOP may catalyze the synthesis of mixed-linkage polyubiquitin chains on HIPK2 and that the K27, K29, K33, K48 and K63 residues in Ub were involved. Similar ubiquitin linkage types were also present in other SPOP-catalyzed substrates, such as with INF2 (20) and MyD88 (21).

Having established that SPOP promoted an atypical ubiquitination of HIPK2, we next sought to identify the ubiquitin attachment sites on HIPK2. We coexpressed FLAG–HIPK2, Myc–SPOP, and HA-Ub in 293T cells and analyzed the immunoprecipitated ubiquitin–HIPK2 conjugates by using mass spectrometry (MS). MS identification revealed that HIPK2 was ubiquitinated at five lysines–K215, K270, K299, K355 and K430 (Figure 2H, I). Interestingly, all these ubiquitin attachment sites were localized in the kinase domain of HIPK2 (Figure 2H). We constructed single K→R or quintuple K→R point mutants of HIPK2 (HIPK2-5KR), and then performed the *in vivo*

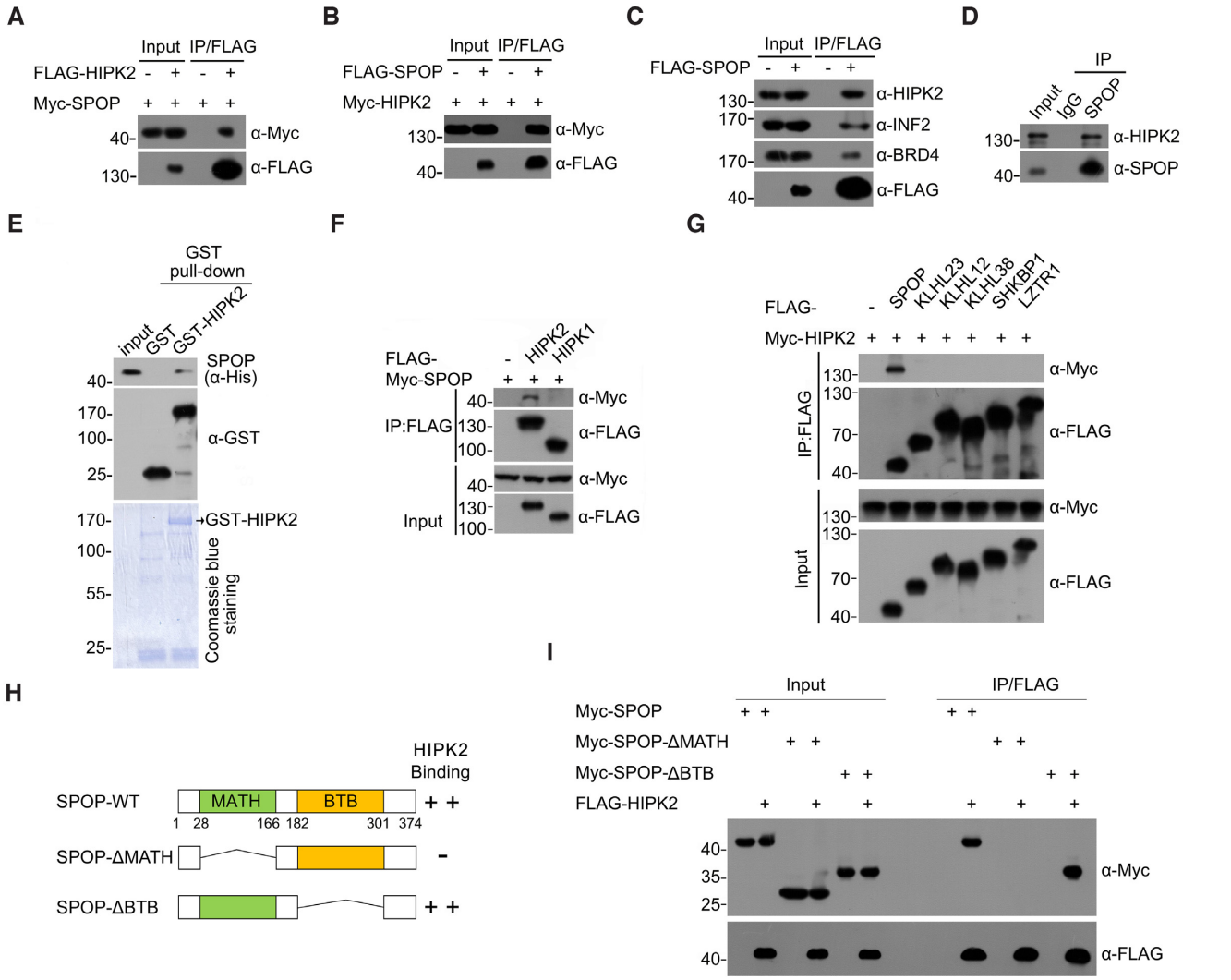

Figure 1. SPOP interacts with HIPK2. (**A**–**C**) Western blot of the indicated proteins in WCLs and co-IP samples of anti-FLAG antibody obtained from 293T cells transfected with indicated plasmids. (**D**) Western blot of the indicated proteins in WCLs and co-IP samples of IgG or anti-SPOP antibody obtained from the cell extracts of PC-3 cells. (**E**) Bacterially expressed GST-HIPK2 proteins or GST bound glutathione-Sepharose beads and incubated with bacterially expressed $(His)_6$-SPOP proteins. Bound $(His)_6$-SPOP proteins were detected by Western blot with anti-His antibody. GST and GST-HIPK2 proteins were detected by western blot and Coomassie Blue staining. (**F**, **G**) Western blot of the indicated proteins in WCLs and co-IP samples of anti-FLAG antibody obtained from 293T cells transfected with indicated plasmids. (**H**) Schematic representation of SPOP deletion mutants. A binding capacity of SPOP to HIPK2 is indicated with the symbol. (**I**) Western blot of the indicated proteins in WCL and co-IP samples of anti-FLAG antibody obtained from 293T cells transfected with indicated plasmids.

ubiquitination assays to evaluate whether these five lysines of HIPK2 were true ubiquitin attachment sites catalyzed by SPOP. To isolate these effects on ubiquitination and not binding, we note that these mutants could still bind to SPOP in a manner similar to that of wild-type HIPK2 (Supplementary Figure S4C). Single K→R mutations considerably reduced HIPK2 ubiquitination, and HIPK2-5KR mutant were unable to be ubiquitinated by SPOP (Figure 2J). We then performed this assay using a reciprocal series of these mutants which only contained only one lysine, with the other four lysines mutated to arginines. The *in vivo* ubiquitination assays showed that these HIPK2 mutants could also be ubiquitinated by SPOP, although the effect was much weaker than that of HIPK2-WT (Figure 2J). Previous studies had shown that the E3 ubiquitin ligases Siah1 and Siah2 can specifically catalyze the degradative ubiquitination on HIPK2 (36,37). We found that HIPK2-5KR mutant could be strongly ubiquitinated by either Siah1 or Siah2 at a level comparable to HIPK2-WT, suggesting that SPOP and Siah1/2 utilize different Ub attachment sites on HIPK2 (Supplementary Figure S4D). Finally, we performed the cycloheximide chase assay to measure the half-life of HIPK2-WT and 5KR mutant in parental or SPOP-KO PC-3 cells and showed these proteins have similar rates of turnover (Supplementary Figure S5A, B). Taken together, our findings suggest that SPOP promotes the atypical non-degradative ubiquitination of HIPK2, and that the five lysines located in the kinase domain of HIPK2 serve as the primary ubiquitin attachment sites.

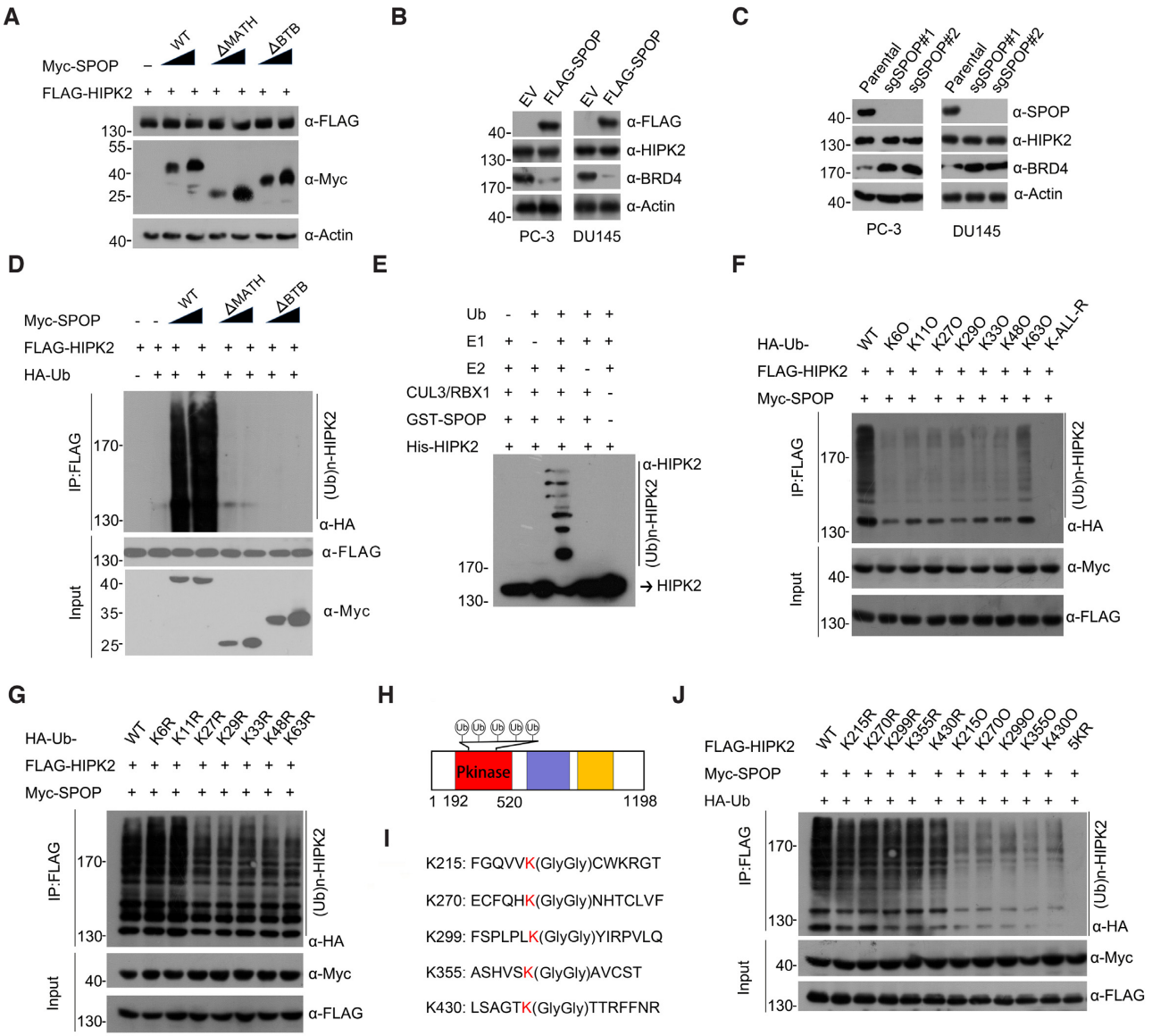

Figure 2. SPOP promotes the non-degradative ubiquitination of HIPK2. (**A**) Western blot of the indicated proteins in WCL from 293T cells transfected with indicated plasmids. (**B**) Western blot of the indicated proteins in WCL from PC-3 or DU145 cells infected with lentivirus expressing empty vector (EV) or FLAG-SPOP. (**C**) Western blot of the indicated proteins in WCL from parental or SPOP knockout PC-3/DU145 cells. (**D**) Western blot of the products of *in vivo* ubiquitination assays from 293T cells transfected with the indicated plasmids. (**E**) Western blot of the products of *in vitro* ubiquitination assays performed by incubating the reconstituted SPOP–CUL3–RBX1 E3 ligase complex with E1 and E2 enzymes, ubiquitin and GST-HIPK2 at 30°C for 2 h. (**F**, **G**) Western blot of the products of *in vivo* ubiquitination assays from 293T cells transfected with the indicated plasmids. (**H**) Schematic representation of HIPK2 domain architecture and Ub indicates ubiquitin attachment sites. (**I**) Identification of ubiquitin attachment sites on HIPK2 (see Materials and methods for details). Tandem mass spectrometry analysis of immunoprecipitated FLAG-HIPK2 showing ubiquitinated peptides. The lysine residues that are ubiquitinated indicates as red. (**J**) Western blot of the products of *in vivo* ubiquitination assays from 293T cells transfected with the indicated plasmids.

Two SPOP-binding consensus motifs in HIPK2 are required for SPOP–HIPK2 binding and SPOP-mediated HIPK2 ubiquitination

Previous studies have reported that one or several SPOP-binding consensus (SBC) motifs (Φ-π-S-S/T-S/T, where Φ: nonpolar residues and π: polar residue) are present in SPOP substrates (4). We examined the HIPK2 protein sequence and identified eight potential SBC motifs (Supplementary Figure S6A). We first generated three deletion mutants of HIPK2 (D1–3) and tested their capabilities to bind SPOP to identify the regions required for the SPOP–HIPK2 interaction (Supplementary Figure S6A). The co-IP assay showed that the N-terminal and C-terminal region, but not the central region of HIPK2 interacted with SPOP, suggesting that more than one SBC motifs were present in HIPK2 (Supplementary Figure S6B). We then generated several point mutants in HIPK2-D1 and D3 to identify the SBC motifs in these two regions that are responsible for the interaction (Supplementary Figure S6A). The co-IP assay showed that ^{97}ASSTS^{101} and ^{863}ASSTT^{867} were required for the binding of HIPK2-D1 and HIPK2-D3 to SPOP, respec-

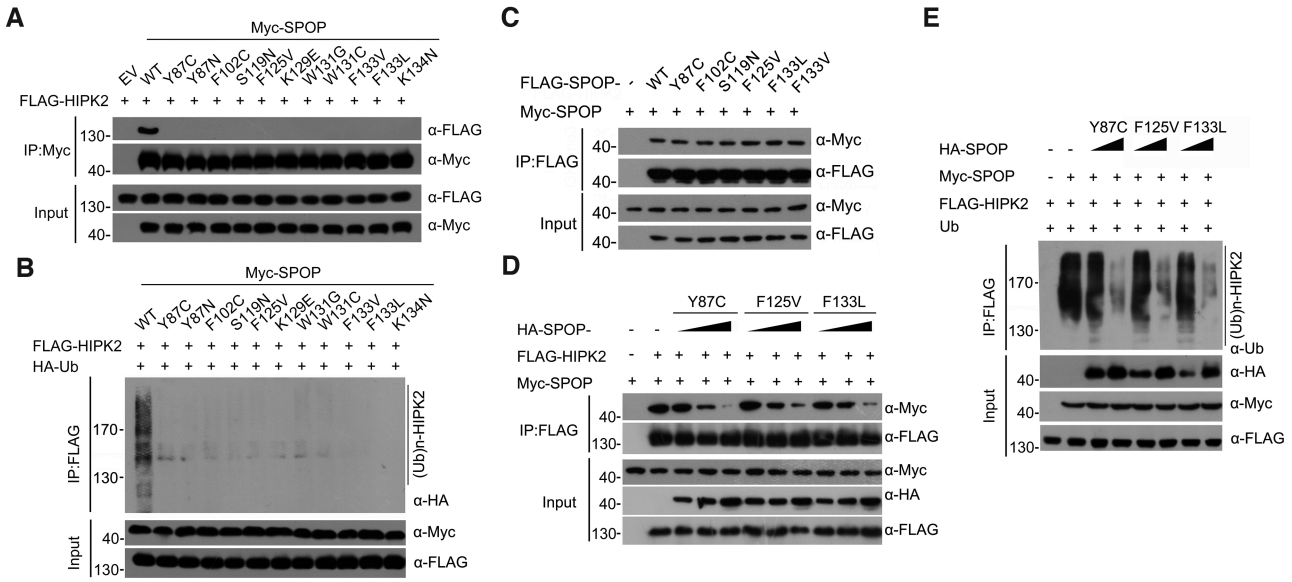

Figure 3. Prostate cancer-associated SPOP mutants are defective in promoting HIPK2 ubiquitination. (**A**) Western blot of WCL and samples from co-IP with anti-FLAG antibody in 293T cells transfected with the indicated plasmids. (**B**) Western blot of the products of *in vivo* ubiquitination assays from 293T cells transfected with the indicated plasmids. (**C**) Western blot of WCL and samples from co-IP with anti-FLAG antibody in 293T cells transfected with the indicated plasmids. (**D**) Western blot of WCL and samples from co-IP with anti-FLAG antibody in 293T cells transfected with the indicated plasmids. (**E**) Western blot of the products of *in vivo* ubiquitination assays from 293T cells transfected with the indicated plasmids.

tively (Supplementary Figure S6C). The point mutations of both motifs in HIPK2 (mSBC) completely abrogated the SPOP–HIPK2 interaction and the SPOP-mediated HIPK2 ubiquitination (Supplementary Figure S6D-F). IF analysis showed that HIPK2-mSBC mutant was not colocalized with SPOP as nuclear puncta in cells (Supplementary Figure S1A). HIPK2-mSBC mutant showed similar rates of turnover as HIPK2-WT (Supplementary Figure S5A, B). Therefore, we have identified the two SBC motifs present in HIPK2 that are essential for HIPK2–SPOP interaction and SPOP-dependent HIPK2 ubiquitination.

Prostate cancer-associated mutants of SPOP are defective in SPOP–HIPK2 interaction and SPOP-mediated HIPK2 ubiquitination

The majority of the SPOP mutations detected thus far in prostate cancer primarily occur in the MATH domain, which is responsible for substrate binding (1). We postulated that the prostate cancer-associated SPOP mutants may be defective in HIPK2 binding. Thus, we examined the interactions between a panel of prostate cancer-associated SPOP mutants and HIPK2 through co-IP assays. As shown in Figure 3A, the binding capability of all SPOP mutants was abolished compared with that of wild-type SPOP. SPOP-mediated HIPK2 ubiquitination was also markedly attenuated for these mutants (Figure 3B). The SPOP mutations are heterozygous missense mutations with a dominant negative selective loss-of-function toward the wild-type allele. We also demonstrated that Pca-associated SPOP mutants dimerized with wild-type SPOP (Figure 3C). In accordance with previous studies (10), our study found that the coexpression of Pca-associated SPOP mutants (Y87C, F125V, or F133L) markedly reduced the interaction between wild-type SPOP and HIPK2 (Figure 3D) and suppressed wild-type SPOP-mediated HIPK2 ubiquitination (Figure 3E). When Pca-associated SPOP mutant, wild-type SPOP and HIPK2 were simultaneously coexpressed in cells, we observed that wild-type SPOP was colocalized with F125V or F133L mutant, but lost the capacity to colocalize with HIPK2, corroborating that these Pca-associated SPOP mutants exerted a dominant negative effect (Supplementary Figure S1B). Taken together, our findings suggest that HIPK2 ubiquitination is dysregulated by oncogenic prostate cancer-associated SPOP mutations.

Functional impact of the SPOP–HIPK2 axis on prostate cancer cell growth

Studies conducted on most cancer cell lines or knockout mice support the notion that HIPK2 generally acts as a tumor suppressor (27). However, the biological function of HIPK2 in prostate cancer remains poorly understood. A previous study showed that HIPK2 enhances the transcriptional activity of androgen receptor (AR), and that HIPK2 knockdown by shRNAs or inhibition by small molecules reduces the proliferation of AR-expressing prostate cancer cells, but does not affect AR-deficient PC-3 cells (38). We ablated HIPK2 expression in two AR-deficient cell lines (PC-3 and DU145) by using CRISPR/Cas9 methods (Supplementary Figures S7, S8), resulting in a marked decrease in cell growth *in vitro* and *in vivo* as determined by CCK-8, colony formation, and xenograft tumor growth assays (Supplementary Figure S9A–H). We found that HIPK2 overexpression also decreased prostate cancer cell growth (Supplementary Figure S9I–N). We further showed that the HIPK2-5KR or mSBC mutant had considerably weaker cell growth-suppressive activity than the

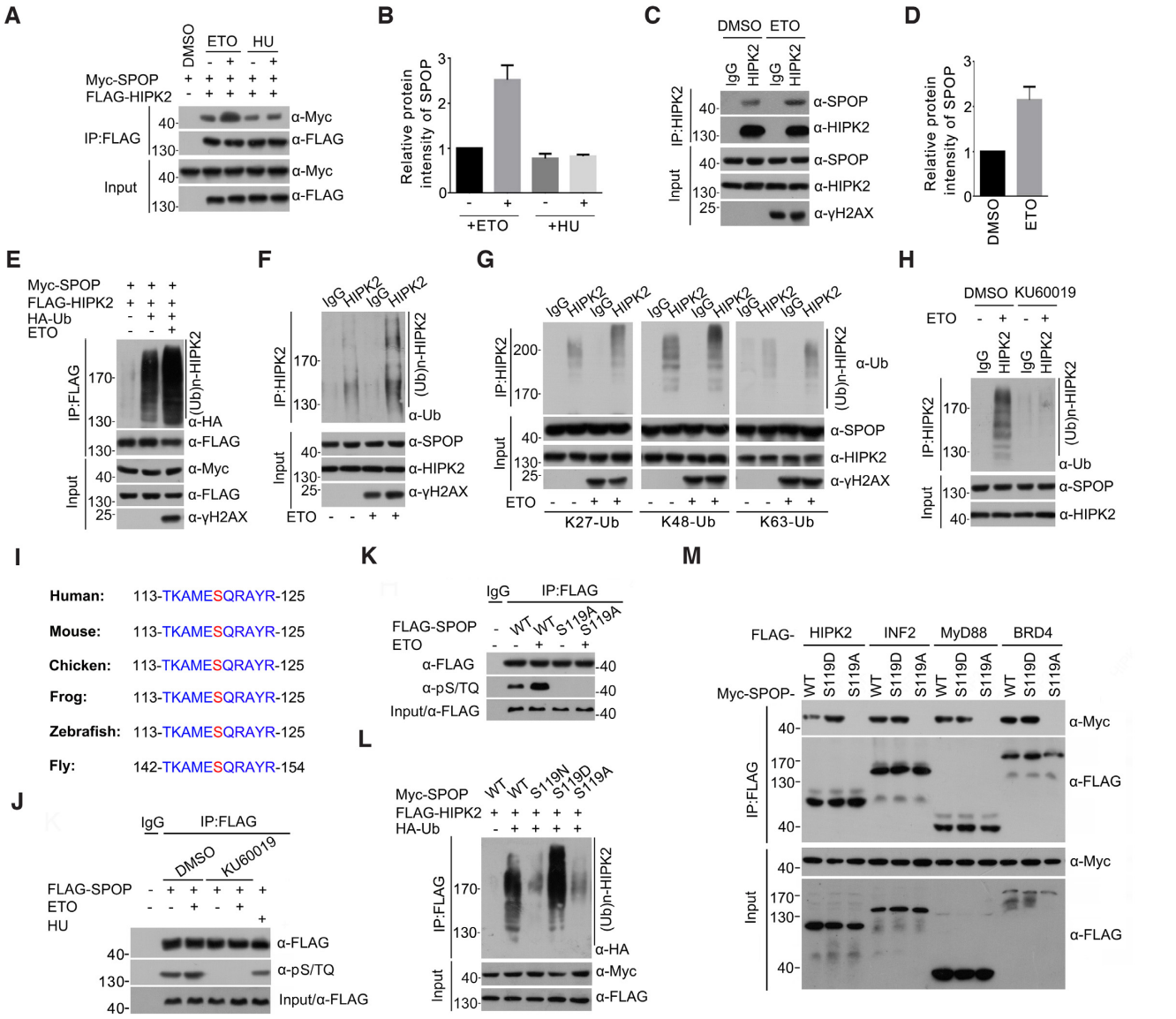

Figure 4. ATM-mediated serine 119 phosphorylation of SPOP augments its capacity to ubiquitinate HIPK2 under genotoxic stress. (**A**) Western blot of WCL and samples from co-IP with anti-FLAG antibody in 293T cells transfected with the indicated plasmids and treated with DMSO, etoposide (75 μg/ml) or hydroxyurea (HU,1 mM) for 4 h. (**B**) Western blot signal intensity of immunoprecipitated Myc-SPOP proteins shown in (A). Band intensity was also quantified by ImageJ. All data shown are mean values ± SD (error bar) from three independent experiments. (**C**) Western blot of the indicated proteins in WCLs and co-IP samples of IgG or anti-HIPK2 antibody obtained from the cell extracts of PC-3 cells treated with DMSO or etoposide (75 μg/ml) for 4 h. (**D**) Western blot signal intensity of immunoprecipitated endogenous SPOP proteins shown in (C). Band intensity was also quantified by ImageJ. All data shown are mean values ± SD (error bar) from three independent experiments. (**E**) Western blot of the products of *in vivo* ubiquitination assays from 293T cells transfected with the indicated plasmids and treated with DMSO or etoposide (75 μg/ml) for 4 h. (**F**) Western blot of WCLs and co-IP samples of IgG or anti-HIPK2 antibody obtained from the cell extracts of PC-3 cells treated with DMSO or etoposide (75 μg/ml) for 4 h. Ub antibody was used to detect the ubiquitinated HIPK2. (**G**) Western blot of WCLs and co-IP samples of IgG or anti-HIPK2 antibody obtained from the cell extracts of PC-3 cells treated with DMSO or etoposide (75 μg/ml) for 4 h. (**H**) Western blot of the indicated proteins in WCLs and co-IP samples of anti-HIPK2 antibody obtained from the cell extracts of PC-3 cells treated with DMSO or etoposide (75 μg/ml) for 4 h in combination of an ATM inhibitor KU60019 (2.5 μM) or not. (**I**) Amino acid sequence alignment of the potential ATM/ATR substrate motif present in SPOP homologs of vertebrates and fruit fly. (**J**) Western blot of WCL and samples from co-IP with IgG or anti-FLAG antibody in control or FLAG-SPOP transfected 293T cells treated with DMSO, etoposide (75 μg/ml), HU(1 mM) for 4 h in combination of an ATM inhibitor KU60019 (2.5 μM) or not. (**K**) Western blot of WCL and samples from co-IP with anti-FLAG antibody in SPOP-WT or mutant-transfected 293T cells treated with etoposide (75 μg/ml) for 4 h. (**L**) Western blot of the products of *in vivo* ubiquitination assays from WCLs and co-IP with anti-FLAG antibody in 293T cells transfected with the indicated plasmids. (**M**) Western blot of WCL and samples from co-IP with anti-FLAG antibody in 293T cells transfected with the indicated plasmids.

wild-type HIPK2 (Supplementary Figure S9I-N), suggesting that SPOP-mediated HIPK2 ubiquitination might potentiate the growth-suppressive function of HIPK2. However, there remains a possibility that the kinase activity of HIPK2 is impaired since the K→R mutations of the five ubiquitin attachment sites are located in the kinase domain. Taken together, our findings suggest that HIPK2 protein levels must be carefully regulated for optimal cancer cell growth.

DNA damage potentiates SPOP-mediated HIPK2 ubiquitination possibly through the phosphorylation of SPOP at Ser119 by ATM

HIPK2 plays a critical role in DNA damage-induced cell fate through the phosphorylation of multiple key cell-cycle regulators (27,28). Thus, we hypothesized that the SPOP–HIPK2 axis may function in DDR. First, we investigated whether the interaction between SPOP and HIPK2 would change following DNA damage. We found that exogenous interactions between SPOP and HIPK2 was enhanced upon a chemotherapy drug etoposide (ETO) treatment which caused DNA double-strand breaks, as demonstrated by co-IP (Figure 4A, B) and in situ proximity ligation assays (Supplementary Figure S1C, D). We also tested hydroxyurea (HU), which causes stalled replication forks and primarily activate the ATR–Chk1 pathway. However, HU treatment had no impact on the SPOP–HIPK2 interaction (Figure 4A, B). ETO treatment also enhanced the endogenous SPOP–HIPK2 interaction (Figure 4C, D). However, ETO treatment had no impact on HIPK2 turnover in presence of SPOP (Supplementary Figure S5C). SPOP-mediated HIPK2 ubiquitination was greatly enhanced upon ETO treatment (Figure 4E). ETO treatment also elevated endogenous HIPK2 ubiquitination levels, as detected by Ub (Figure 4F) or Ub linkage-specific (K27, K48 or K63) antibodies (Figure 4G). A previous study showed that SPOP specifically interacted with the ATM serine/threonine kinase upon IR-induced DNA damage (39). We found that pretreating the cells with the ATM-specific inhibitor KU60019 remarkably reduced DNA damage-induced HIPK2 ubiquitination (Figure 4H). Considering that ATM might directly phosphorylate SPOP, we searched for potential phosphorylation sites that conformed to the ATM S/T-Q consensus motif on SPOP. Although three S/T-Q motifs were present in the SPOP protein sequence, the second motif, ^{119}SQ^{120}, was of primary interest because it is located at the substrate-binding MATH domain and highly conserved among SPOP orthologues, ranging from human to fly (Figure 4I). Interestingly, SPOP S119N mutation recurrently occurred in prostate cancers (3). We immunoprecipitated ectopically expressed SPOP in 293T cells treated with DMSO or ETO, and detected possible ATM-mediated SPOP phosphorylation by using a phospho-S/TQ motif antibody. ETO treatment resulted in a profound elevation of phospho-S/TQ SPOP signals that is eliminated by an ATM inhibitor pretreatment. In contrast, HU treatment had no impact on phospho-S/TQ SPOP signals. Weak phospho-S/TQ SPOP signals were detected in untreated cells but eliminated by an ATM inhibitor, suggesting that SPOP can be phosphorylated by basal ATM activity (Figure 4J). An S119A mutation in SPOP completely abolished the DNA damage-induced phospho-S/TQ signal (Figure 4K). We showed that the phospho-mimic mutant SPOP-S119D exerted a stronger impact on HIPK2 ubiquitination than SPOP-WT; by contrast, the dephospho-mimic mutant SPOP-S119A completely lost its capacity to ubiquitinate HIPK2 (Figure 4L). IF analysis showed that SPOP-S119D, but not S119A mutant, was colocalized with HIPK2 in nuclear bodies(Supplementary Figure S1A). Co-IP assays results showed that SPOP-S119D mutant showed stronger binding affinity towards HIPK2 than wild-type SPOP (Figure 4M). We also detected the interaction between SPOP-WT/S119A/S119D and other reported SPOP substrates (MyD88, INF2, and BRD4). In contrast to HIPK2, SPOP-S119D showed similar binding affinity towards INF2, MyD88, and BRD4, as wild-type SPOP, implying that ATM-mediated phosphorylation may increase SPOP's affinity towards a subset, but not all substrates (Figure 4M). Taken together, our results suggest that ATM-mediated phosphorylation of SPOP at Ser119 contributes to HIPK2 ubiquitination upon DNA damage.

Functional effect of the SPOP–HIPK2 axis in DNA damage-induced cell death

HIPK2 has been reported to promote DNA damage-induced apoptosis in both a p53-dependent or p53-independent manner (27). By contrast, HIPK2 also alleviates sub-lethal UV-induced apoptosis by promoting the DDR (29). Therefore, we sought to examine whether SPOP-mediated HIPK2 ubiquitination would affect DDR and ultimately cellular sensitivity to genotoxic agents in prostate cancer cells. We treated parental or HIPK2-KO PC-3 cells with ETO for 24 h and then allowed the cells to recover for the indicated durations in drug-free media. The Ser139 phosphorylation of H2AX (γH2AX), a cellular response to the induction of DNA double-stranded breaks, was assessed via Western blot analysis. As shown in Figure 5A, in parental PC-3 cells, the γH2AX signal was completely eliminated at 24 h after recovery, suggesting a successful DNA repair. By contrast, in HIPK2-KO PC-3 cells, a strong γH2AX signal persisted 24 h after recovery, suggesting that HIPK2 is essential for ETO-induced DDR and repair (Figure 5A). Similar results were obtained from HIPK2-KO DU145 cells (Supplementary Figure S10A). However, IF analysis showed that SPOP/HIPK2 puncta were not colocalized with γH2AX foci (Supplementary Figure S1E).

We reconstituted the expression of HIPK2-WT, -mSBC, -5KR or -kinase dead (KD, K228R mutation) mutant in HIPK2-KO PC-3 cells to further dissect whether SPOP-mediated HIPK2 ubiquitination was implicated in DDR. Before that, we tested whether HIPK2-5KR mutations had any impact on the kinase activity since these mutated lysine residues are located in the kinase domain of HIPK2. However, co-expression of HIPK2-WT or HIPK2-5KR mutant with p53 led to a similar increase in the phospho-p53 (Ser46) signal levels (Supplementary Figure S11A). Similar results were obtained by *in vitro* kinase assays using recombinant p53 as a substrate (Supplementary Figure S11B). These results indicated that HIPK2-5KR mutations had no obvious impact on the basal kinase activity of HIPK2.

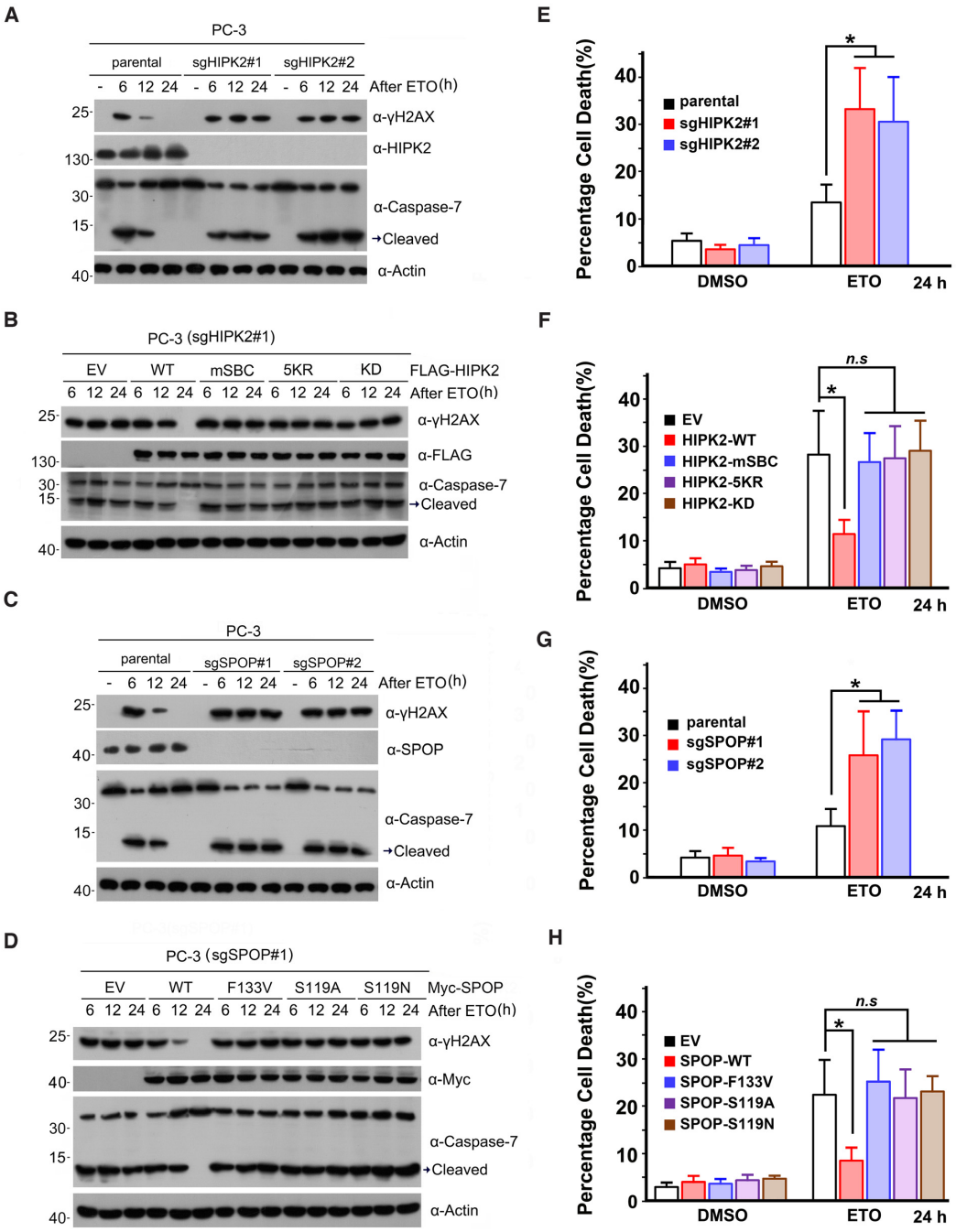

Figure 5. The critical role of SPOP-HIPK2 axis in genotoxic stress-induced cell death. (**A**) Parental and HIPK2-KO PC-3 cells were treated with etoposide (75 μg/ml) for 24 h, then the treatment media is removed and replaced with fresh media for indicated times. The WCL were prepared for Western blot. The DMSO-treated cells were used as a control. (**B**) HIPK2-KO PC-3 cells stably expressing EV, HIPK2-WT, mSBC, 5KR, or KD mutant, were treated with etoposide (75 μg/ml) for 24 h, then the treatment media is removed and replaced with fresh media for indicated times. The WCL were prepared for western blot. (**C**) Parental and SPOP-KO PC-3 cells were treated with etoposide (75 μg/ml) for 24 h, then the treatment media is removed and replaced with fresh media for indicated times. The WCL were prepared for western blot. The DMSO-treated cells were used as a control. (**D**) SPOP-KO PC-3 cells stably expressing EV, SPOP-WT, -F133V, -S119A or -S119N mutant were treated with etoposide (75 μg/ml) for 24 h, then the treatment media is removed and replaced with fresh media for indicated times. The WCL were prepared for western blot. The DMSO-treated cells were used as a control. (**E**) Cell death analysis (PI staining) of parental and HIPK2-KO PC-3 cells treated with DMSO or etoposide (75 μg/ml) for 24 h. All data shown are mean values ± SD (error bar) from three independent experiments. $^{*}P < 0.05$, calculated using the Student's *t* test. (**F**) Cell death analysis of HIPK2-KO PC-3 cells stably expressing EV, HIPK2-WT, -mSBC, -5KR, -KD mutant, treated with DMSO or etoposide (75 μg/ml) for 24 h. All data shown are mean values ± SD (error bar) from three independent experiments. $^{*}P < 0.05$, calculated using the Student's *t* test. (**G**) Cell death analysis of parental and SPOP-KO PC-3 cells treated with DMSO or etoposide (75 μg/ml) for 24 h. All data shown are mean values ± SD (error bar) from three independent experiments. $^{*}P < 0.05$, calculated using the Student's *t* test. (**H**) Cell death analysis of SPOP-KO PC-3 cells stably expressing EV, SPOP-WT or -F133V, -S119A or -S119N mutant, treated with etoposide (75 μg/ml) for 24 h. All data shown are mean values ± SD (error bar) from three independent experiments. $^{*}P < 0.05$, calculated using the Student's *t* test.

We found that the stable overexpression of HIPK2-WT in HIPK2-KO PC-3 cells restored γH2AX clearance during recovery. By contrast, HIPK2-mSBC, -5KR or -KD mutant-overexpressed cells still exhibited defective γH2AX clearance (Figure 5B). Similar results were obtained from HIPK2-KO DU145 cells reconstituted with HIPK2-WT, -mSBC, -5KR or -KD mutant (Supplementary Figure S10B). In accordance with studies reporting on impaired DDR in SPOP-deficient cells (24), we found that SPOP-KO DU145/PC-3 cells exhibited a defective γH2AX clearance that could be rescued by the stable overexpression of wild-type SPOP, but not by that of the F133V, S119A or S119N mutant (Figure 5C, D; Supplementary Figure S10C, D). To assess the effect of SPOP-HIPK2 axis on DDR *in vivo*, we performed the alkaline Comet assay, which is an sensitive technique for the detection of DNA damage at the level of the individual cells. Single PC-3 cell suspensions are embedded in agarose before subjecting to electrophoresis. As damaged DNA migrates faster, nuclei with DNA damage exhibit a comet-like morphology, with longer length of the DNA in the comet 'tail' indicating increased DNA damage and quantified as 'tail moment'. As shown in Figure 6A–D, the comet-like morphology of nuclei was completely eliminated at 24 h after recovery in paternal PC-3 cells or SPOP, HIPK2-KO PC-3 cells that were reconstituted with SPOP-WT or HIPK2-WT, respectively. By contrast, SPOP-KO cells and cells that were reconstituted with SPOP-F133V, -S119A or -S119N mutant, HIPK2-KO cells that were reconstituted with SPOP-mSBC, -5KR or KD mutant, were all showed comet-like morphology of nuclei at 24 h after recovery. Collectively, these results suggest that the integrity of SPOP-HIPK2 axis is indispensable for timely DNA damage repair in cells.

Given that HIPK2 or SPOP ablation impaired the DDR, cells lacking HIPK2 or SPOP were expected to show increased sensitivity to DNA damage-induced cell death. Indeed, ETO-induced cell death was more evident in HIPK2-KO or SPOP-KO DU145/PC-3 cells than in their respective parental cells, as demonstrated by Caspase-7 cleavage or FACS with propidium iodide staining (Figure 5A, C, E, G; Supplementary Figure S10A, C, E, G). Moreover, we found that the stable overexpression of HIPK2-WT, but not that of the -5KR, -mSBC or KD mutant, in HIPK2-KO PC-3/DU145 cells alleviated ETO-induced cell death (Figure 5B, F; Supplementary Figure S10B, F). The stable overexpression of SPOP-WT, but not that of the -F133V, -S119A or -S119N mutant, in SPOP-KO PC-3/DU145 cells alleviated ETO-induced cell death (Figure 5D, H; Supplementary Figure S10D, H). Taken together, our findings suggest that the activation of the SPOP–HIPK2 regulatory axis might directly control the DDR to ensure cell protection after a genotoxic event.

SPOP-mediated HIPK2 ubiquitination augments the capacity to phosphorylate HP1γ and trigger the release of HP1γ from histone H3K9me3

HIPK2-dependent phosphorylation of HP1γ participates in the regulation of the dynamic interaction between HP1γ and histone H3K9me3 to promote DNA damage repair (29). We sought to investigate whether SPOP acts as an upstream regulator of this process. WB analysis showed that HIPK2-KO or SPOP-KO PC-3 cells showed impaired HP1γ phosphorylation elicited by ETO treatment, as determined through a differential migration assay on phos-tag-containing gels (Figure 7A, B). We also showed that in HIPK2-KO PC-3 cells, the stable overexpression of wild-type HIPK2, but not that of the -mSBC, -5KR or KD mutant, restored ETO-elicited HP1γ phosphorylation (Figure 7C). Similarly, the stable overexpression of wild-type SPOP, but not that of the -F133V, -S119A or -S119N mutant, restored ETO-elicited HP1γ phosphorylation (Figure 7D).

HIPK2 regulates the association between HP1γ and histone H3K9me3 upon DNA damage (29). A co-IP assay with an anti-histone H3K9me3 antibody showed that the stable overexpression of wild-type HIPK2, but not that of the -mSBC, -5KR or -KD mutant, triggered the release of HP1γ from histone H3K9me3 in ETO-treated HIPK2-KO PC-3 cells (Figure 7E, F). Similarly, in ETO-treated SPOP-KO PC-3 cells, the stable overexpression of SPOP-WT, but not that of the -F133V, -S119A or -S119N mutant, triggered the release of HP1γ from histone H3K9me3 (Figure 7G). This critical role of the SPOP–HIPK2 axis in regulating DNA-damage-induced HP1γ phosphorylation and HP1γ release from histone H3K9me3 was also found in DU145 cells (Supplementary Figure S12). Taken together, these results suggest that SPOP promotes DNA damage repair, at least in part, by regulating the HIPK2-dependent phosphorylation of HP1γ, which regulates the dynamic interaction between HP1γ and the histone H3K9me3.

DISCUSSION

The functional effect of SPOP mutations on prostate cancer tumorigenesis and progression has been extensively studied in recent years. Although dozens of oncoproteins have been identified as SPOP substrates, the direct molecular mediators through which SPOP exerts its role in safeguarding genome stability remain poorly understood. In this study, we reveal that the DNA damage-responsive kinase, HIPK2, is a *bona fide* SPOP substrate. Mechanistically, DNA damage triggers an ATM-dependent phosphorylation at Ser119 in SPOP, which enhances SPOP's capacity to promote the nondegradative ubiquitination and activation of HIPK2. Subsequently, HIPK2 phosphorylates HP1γ and facilitates HP1γ's release from histone H3K9me3 to promote DNA repair. In addition to SPOP, ATM was reported to promote HIPK2 activation through phosphorylation of E3 ligase Siah-1 at Ser 19 and regulation of HIPK2–Siah-1 interaction (36,40). Given that this signaling cascade is disrupted by prostate cancer-associated SPOP mutations, we propose that dysregulation of this pathway may partially account for the high genomic instability observed in SPOP-mutated subtypes of prostate cancer (Figure 7H).

The epigenetic regulator HP1 proteins HP1α, HP1β and HP1γ are the main components of constitutive heterochromatin, and they contain a chromodomain that recognizes dimethylated or trimethylated lysine 9 of histone H3 (H3K9me2 and H3K9Me3) (41). HP1 proteins have been established as key players in many aspects of DDR. Some studies suggest that HP1 proteins are released from histone H3K9me3 to promote the recruitment of DDR fac-

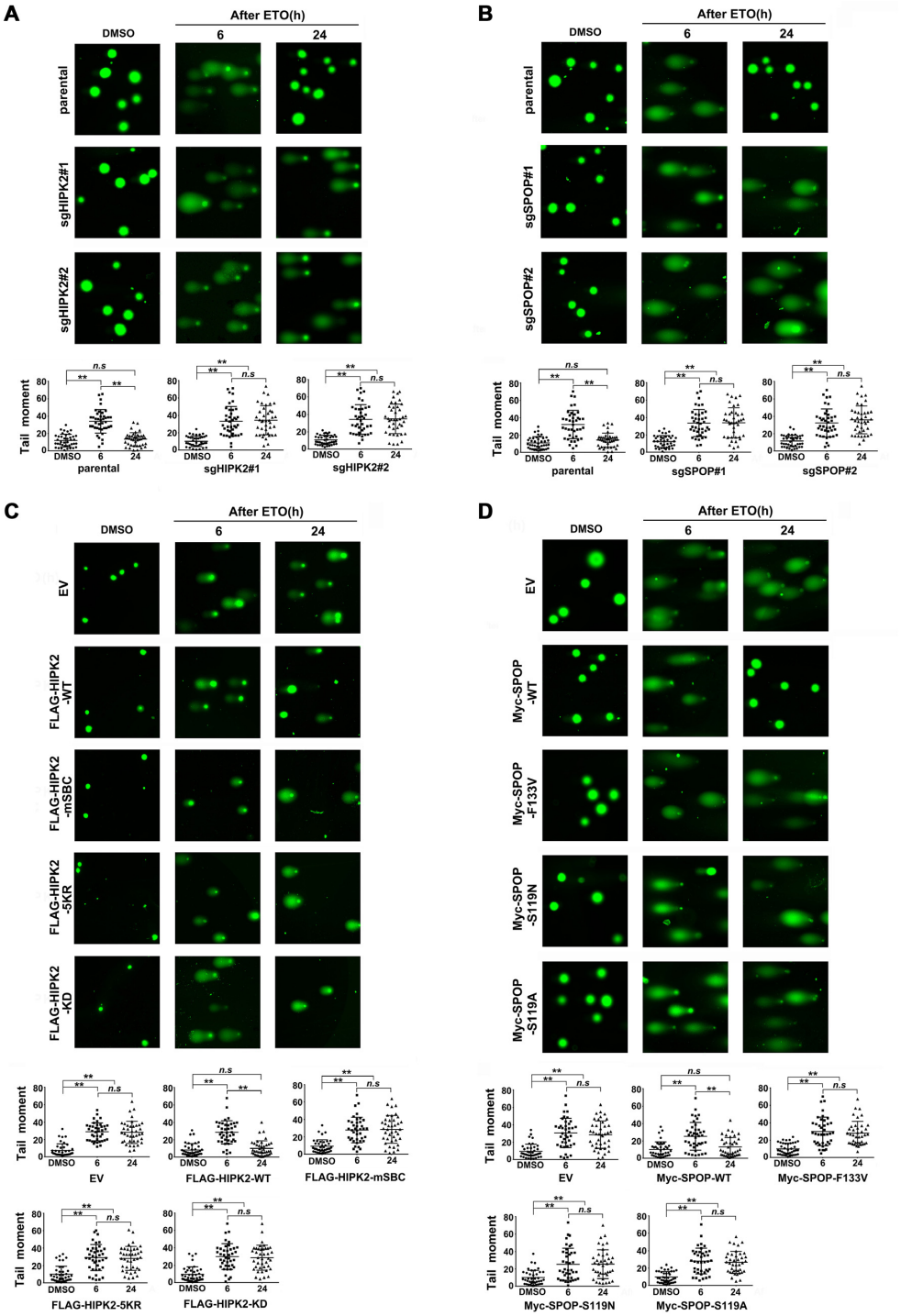

Figure 6. Assessment the effect of SPOP-HIPK2 axis on DNA damage repair in vivo by comet assays. (**A**) Parental and HIPK2-KO PC-3 cells were treated with etoposide (75 μg/ml) for 24 h, then the treatment media is removed and replaced with fresh media for indicated times. The comet assays were then performed and 40 cells from each sample were analyzed based on the tail moment, utilizing the Komet software. All data shown are mean values ± SD (error bar). $^{**}P < 0.01$, calculated using the Student's *t* test. (**B**) Parental and SPOP-KO PC-3 cells were treated with etoposide (75 μg/ml) for 24 h, then the treatment media is removed and replaced with fresh media for indicated times. The comet assays were then performed and 40 cells from each sample were analyzed based on the tail moment, utilizing the Komet software. All data shown are mean values ± SD (error bar). $^{**}P < 0.01$, calculated using the Student's *t* test. (**C**) Parental and HIPK2-KO PC-three cells stably expressing EV, HIPK2-WT, -mSBC, -5KR or -KD mutant were treated with etoposide (75 μg/ml) for 24 h, then the treatment media is removed and replaced with fresh media for indicated times. The comet assays were then performed and 40 cells from each sample were analyzed based on the tail moment, utilizing the Komet software. All data shown are mean values ± SD (error bar). $^{**}P < 0.01$, calculated using the Student's *t* test. (**D**) Parental and SPOP-KO PC-3 cells stably expressing EV, SPOP-WT, -F133V, -S119A or -S119N mutant were treated with etoposide (75 μg/ml) for 24 h, then the treatment media is removed and replaced with fresh media for indicated times. The comet assays were then performed and 40 cells from each sample were analyzed based on the tail moment, utilizing the Komet software. All data shown are mean values ± SD (error bar). $^{**}P < 0.01$, calculated using the Student's *t* test.

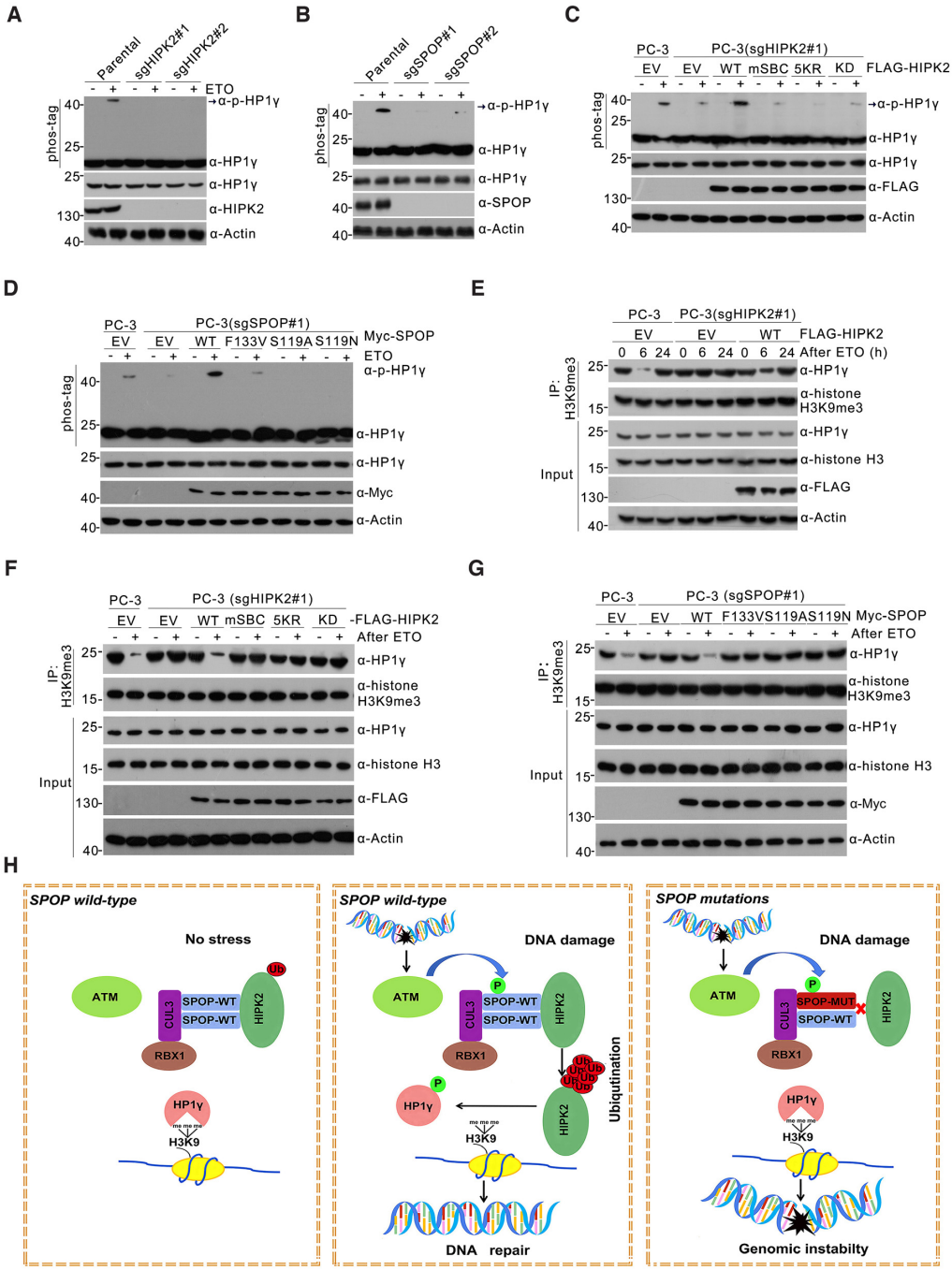

Figure 7. The critical role of SPOP-HIPK2 axis in regulation of HP1γ binding to histone H3K9me3 under genotoxic stress. (**A**) Western blot of WCL from parental and HIPK2-KO PC-3 cells treated with DMSO or etoposide (75 μg/ml) for 24 h. The phosphorylated form of HP1γ (p-HP1γ) was detected by phos-tag SDS-PAGE using an anti-HP1γ antibody. (**B**) Western blot of WCL from parental and SPOP-KO PC-3 cells treated with DMSO or etoposide (75 μg/ml) for 24 h. The phosphorylated form of HP1γ (p-HP1γ) was detected by phos-tag SDS-PAGE using an anti-HP1γ antibody. (**C**) Western blot of WCL from HIPK2-KO PC-3 cells stably expressing EV, HIPK2-WT, or mutants, treated with etoposide (75 μg/ml) for 24 h.The phosphorylated form of HP1γ (p-HP1γ) was detected by phos-tag SDS-PAGE using an anti-HP1γ antibody. (**D**) Western blot of WCL from SPOP-KO PC-3 cells stably expressing EV, SPOP-WT, or mutants, treated with etoposide (75 μg/ml) for 24 h. The phosphorylated form of HP1γ (p-HP1γ) was detected by phos-tag SDS-PAGE using an anti-HP1γ antibody. (**E**) Parental and HIPK2-KO PC-3 cells were treated with etoposide (75 μg/ml) for 24 h, then the treatment media is removed and replaced with fresh media for indicated times. The WCL were prepared for co-IP with anti-histone H3K9me3 antibody. The WCL and co-IP samples were detected by western blot. (**F**) Parental and HIPK2-KO PC-3 cells stably expressing EV, HIPK2-WT, or mutants were treated with etoposide (75 μg/ml) for 24 h, then the treatment media is removed and replaced with fresh media for 6 h. The WCL were prepared for co-IP with anti-histone H3K9me3 antibody. The WCL and co-IP samples were detected by western blot. The DMSO-treated cells were used as a control (–). (**G**) Parental and SPOP-KO PC-3 cells stably expressing EV, SPOP-WT, or mutants were treated with etoposide (75 μg/ml) for 24 h, then the treatment media is removed and replaced with fresh media for 6 h. The WCL were prepared for co-IP with anti-histone H3K9me3 antibody. The WCL and co-IP samples were detected by western blot. The DMSO-treated cells were used as a control (–). (**H**) Schematic of the proposed mechanism through which SPOP mutants trigger the genomic instability in SPOP-mutated prostate cancer.

tors to DNA lesions, whereas other studies have reached the opposite conclusion (42). The signaling pathway that controls for spatial localization and temporal dynamics of HP1 upon DNA damage remains poorly understood. Upon sublethal UV irradiation, HIPK2 is activated to phosphorylate HP1γ, which causes the dissociation of HP1γ at damaged DNA sites (29). Our results suggest that SPOP or HIPK2 is also required for HP1γ phosphorylation and subsequent DDR in chemotherapy drug-treated prostate cancer cells.

The protein level and activity of HIPK2 is dynamically regulated by various post-transcriptional modifications under various environmental stresses (28). HIPK2 protein levels are regulated by the degradative ubiquitination pathway, involving at least five reported E3 ubiquitin ligases–Siah1, Siah2, Fbx3, WSB1 and Mdm2 (28). Previous studies have shown that when the ubiquitination of HIPK2 is suppressed, HIPK2 becomes stabilized and triggers p53-dependent apoptosis upon lethal DNA damage (36,43). However, in at least two p53-deficient prostate cancer cell lines, we did not observe that a lethal dose of ETO treatment affected HIPK2 protein levels. These discrepancies may be due to the cellular systems and experimental conditions used in different studies. To our knowledge, we are first to report here that HIPK2 activity is regulated by non-degradative ubiquitination. Different Ub-linkage types and ubiquitin attachment sites may determine the various cellular fates of modified HIPK2. Our results show that simultaneous mutations at five lysine residues in the kinase domain of HIPK2 completely abolishes SPOP-mediated HIPK2 ubiquitination. However, Siah1 or Siah2 -mediated HIPK2 ubiquitination was largely unaffected. In contrast to degradative ubiquitination that usually displays promiscuity at multiple ubiquitination sites, non-degradative ubiquitination typically modulates protein structure, dynamics, and function, and these ubiquitin attachment sites may be confined to specific lysines that are crucial to molecular functions. The molecular mechanisms underlying the enhancement of HIPK2 activity by SPOP-mediated ubiquitination remain unclear. We suspected that this kind of ubiquitination may lead to a conformational change, which facilitates HIPK2 auto-phosphorylation and subsequent activation (44). Another possibility is that the ubiquitin chain may also act as a platform for recruiting various scaffold and accessory proteins, such as Han11 and Pin1, to control the threshold, amplitude, and kinetics of HIPK2-triggered signaling transduction (44,45). Nevertheless, the exact mechanisms by which ubiquitination modulates HIPK2 activity remain to be elucidated in future work.

Notably, the regulatory role of SPOP in response to DNA damage may not be solely attributed by its activity toward HIPK2. Known substrates degraded by SPOP, such as BRD4, have been reported to function in DDR. BRD4 depletion results in a relaxed chromatin structure, rapid cell-cycle checkpoint recovery, and enhanced survival after DNA damage (46). However, we did not find changes in protein level of BRD4 in ETO-treated PC-3/DU145 cells (data not shown). This could be due to Ser119 phosphorylation in SPOP enhancing its binding affinity towards a subset of substrates, such as HIPK2, but not all substrates. An alternative explanation is that only a small pool of SPOP is phosphorylated and activated upon DNA damage. Therefore, the changes in protein levels of degradative substrates are minimal. Nevertheless, there remains a possibility that SPOP modulates DDR through other known or unidentified substrates.

The post-translational modification of SPOP is poorly understood. A recent report revealed that CDK4/6-mediated SPOP phosphorylation increases the interaction of SPOP with 14–3-3γ, which protects SPOP from Cdh1-mediated proteasomal degradation (14). Our results suggest that the ATM-mediated SPOP phosphorylation at Ser119, which is located in the substrate-binding MATH domain, alters the binding affinity between SPOP and HIPK2. Ser119 phosphorylation likely causes a conformational change in the MATH domain of SPOP to potentiate HIPK2 binding, although this conjecture remains to be experimentally validated in future structural biology study.

DATA AVAILABILITY

All data needed to evaluate the conclusions in the paper are present in the paper and/or the Supplementary Materials. Additional data related to this paper may be requested from the authors.

SUPPLEMENTARY DATA

Supplementary Data are available at NAR Online.

ACKNOWLEDGEMENTS

We thank Dr Lienhard Schmitz (Justus-Liebig-University) for providing HIPK2 constructs.
Author contributions: X.J., C.W. and K.G conceived the study. X.J., Q.S., Q.L., H.Z., L.S., JH.L., H.Q., J.Y., T.L., Z.L., J.W., L.C. and Y.M. performed the experiments and data analyses. C.W., X.J., K.G., Q.M., Y.X., S.F., XY.C., X.M. and Z.G. analyzed and interpreted the data. X.J., C.W., K.G. and S.W. wrote the manuscript.

FUNDING

National Natural Science Foundation of China [31801165 to X.J.,91954106, 81872109 to K.G., 81972396, 91957125 to C.W.]; Natural Science Foundation of Zhejiang Province [LY20C070001 to X.J.]; Natural Science Foundation of Ningbo [2018A610213 to X.J.]; Natural Science Foundation of Shanghai [18ZR1430100 to K.G.]; Program of 'Xinmiao' (Potential) Talents in Zhejiang Province [2019R405061 to J.W., 2019R405011 to Q.L.]; Student Research and Innovation Program of Ningbo University [2018-SRIP1925 to Q.L., 2019SRIP1907 to J.W.]; K.C. Wong Magna Fund in Ningbo University. Funding for open access charge: National Natural Science Foundation of China.
Conflict of interest statement. None declared.

REFERENCES

1. Barbieri,C.E., Baca,S.C., Lawrence,M.S., Demichelis,F., Blattner,M., Theurillat,J.P., White,T.A., Stojanov,P., Van Allen,E., Stransky,N. *et al.* (2012) Exome sequencing identifies recurrent SPOP, FOXA1 and MED12 mutations in prostate cancer. *Nat. Genet.*, **44**, 685–689.

2. Cancer Genome Atlas Research, N. (2015) The molecular taxonomy of primary prostate cancer. *Cell*, **163**, 1011–1025.
3. Blattner,M., Lee,D.J., O'Reilly,C., Park,K., MacDonald,T.Y., Khani,F., Turner,K.R., Chiu,Y.L., Wild,P.J., Dolgalev,I. *et al.* (2014) SPOP mutations in prostate cancer across demographically diverse patient cohorts. *Neoplasia*, **16**, 14–20.
4. Zhuang,M., Calabrese,M.F., Liu,J., Waddell,M.B., Nourse,A., Hammel,M., Miller,D.J., Walden,H., Duda,D.M., Seyedin,S.N. *et al.* (2009) Structures of SPOP-substrate complexes: insights into molecular architectures of BTB-Cul3 ubiquitin ligases. *Mol. Cell*, **36**, 39–50.
5. Li,C., Ao,J., Fu,J., Lee,D.F., Xu,J., Lonard,D. and O'Malley,B.W. (2011) Tumor-suppressor role for the SPOP ubiquitin ligase in signal-dependent proteolysis of the oncogenic co-activator SRC-3/AIB1. *Oncogene*, **30**, 4350–4364.
6. An,J., Wang,C., Deng,Y., Yu,L. and Huang,H. (2014) Destruction of full-length androgen receptor by wild-type SPOP, but not prostate-cancer-associated mutants. *Cell Rep.*, **6**, 657–669.
7. Geng,C., Rajapakshe,K., Shah,S.S., Shou,J., Eedunuri,V.K., Foley,C., Fiskus,W., Rajendran,M., Chew,S.A., Zimmermann,M. *et al.* (2014) Androgen receptor is the key transcriptional mediator of the tumor suppressor SPOP in prostate cancer. *Cancer Res.*, **74**, 5631–5643.
8. An,J., Ren,S., Murphy,S.J., Dalangood,S., Chang,C., Pang,X., Cui,Y., Wang,L., Pan,Y., Zhang,X. *et al.* (2015) Truncated ERG oncoproteins from TMPRSS2-ERG fusions are resistant to SPOP-Mediated proteasome degradation. *Mol. Cell*, **59**, 904–916.
9. Gan,W., Dai,X., Lunardi,A., Li,Z., Inuzuka,H., Liu,P., Varmeh,S., Zhang,J., Cheng,L., Sun,Y. *et al.* (2015) SPOP promotes ubiquitination and degradation of the ERG oncoprotein to suppress prostate cancer progression. *Mol. Cell*, **59**, 917–930.
10. Theurillat,J.P., Udeshi,N.D., Errington,W.J., Svinkina,T., Baca,S.C., Pop,M., Wild,P.J., Blattner,M., Groner,A.C., Rubin,M.A. *et al.* (2014) Prostate cancer. Ubiquitylome analysis identifies dysregulation of effector substrates in SPOP-mutant prostate cancer. *Science*, **346**, 85–89.
11. Dai,X., Gan,W., Li,X., Wang,S., Zhang,W., Huang,L., Liu,S., Zhong,Q., Guo,J., Zhang,J. *et al.* (2017) Prostate cancer-associated SPOP mutations confer resistance to BET inhibitors through stabilization of BRD4. *Nat. Med.*, **23**, 1063–1071.
12. Janouskova,H., El Tekle,G., Bellini,E., Udeshi,N.D., Rinaldi,A., Ulbricht,A., Bernasocchi,T., Civenni,G., Losa,M., Svinkina,T. *et al.* (2017) Opposing effects of cancer-type-specific SPOP mutants on BET protein degradation and sensitivity to BET inhibitors. *Nat. Med.*, **23**, 1046–1054.
13. Zhang,P., Wang,D., Zhao,Y., Ren,S., Gao,K., Ye,Z., Wang,S., Pan,C.W., Zhu,Y., Yan,Y. *et al.* (2017) Intrinsic BET inhibitor resistance in SPOP-mutated prostate cancer is mediated by BET protein stabilization and AKT-mTORC1 activation. *Nat. Med.*, **23**, 1055–1062.
14. Zhang,J., Bu,X., Wang,H., Zhu,Y., Geng,Y., Nihira,N.T., Tan,Y., Ci,Y., Wu,F., Dai,X. *et al.* (2018) Cyclin D-CDK4 kinase destabilizes PD-L1 via cullin 3-SPOP to control cancer immune surveillance. *Nature*, **553**, 91–95.
15. Zhu,H., Ren,S., Bitler,B.G., Aird,K.M., Tu,Z., Skordalakes,E., Zhu,Y., Yan,J., Sun,Y. and Zhang,R. (2015) SPOP E3 ubiquitin ligase adaptor promotes cellular senescence by degrading the SENP7 deSUMOylase. *Cell Rep.*, **13**, 1183–1193.
16. Geng,C., Kaochar,S., Li,M., Rajapakshe,K., Fiskus,W., Dong,J., Foley,C., Dong,B., Zhang,L., Kwon,O.J. *et al.* (2017) SPOP regulates prostate epithelial cell proliferation and promotes ubiquitination and turnover of c-MYC oncoprotein. *Oncogene*, **36**, 4767–4777.
17. Ju,L.G., Zhu,Y., Long,Q.Y., Li,X.J., Lin,X., Tang,S.B., Yin,L., Xiao,Y., Wang,X.H., Li,L. *et al.* (2019) SPOP suppresses prostate cancer through regulation of CYCLIN E1 stability. *Cell Death Differ.*, **26**, 1156–1168.
18. Wang,X., Jin,J., Wan,F., Zhao,L., Chu,H., Chen,C., Liao,G., Liu,J., Yu,Y., Teng,H. *et al.* (2019) AMPK promotes SPOP-mediated NANOG degradation to regulate prostate cancer cell stemness. *Dev. Cell*, **48**, 345–360.
19. Zhang,J., Chen,M., Zhu,Y., Dai,X., Dang,F., Ren,J., Ren,S., Shulga,Y.V., Beca,F., Gan,W. *et al.* (2019) SPOP promotes nanog destruction to suppress stem cell traits and prostate cancer progression. *Dev. Cell*, **48**, 329–344.
20. Jin,X., Wang,J., Gao,K., Zhang,P., Yao,L., Tang,Y., Tang,L., Ma,J., Xiao,J., Zhang,E. *et al.* (2017) Dysregulation of INF2-mediated mitochondrial fission in SPOP-mutated prostate cancer. *PLos Genet.*, **13**, e1006748.
21. Jin,X., Shi,Q., Li,Q., Zhou,L., Wang,J., Jiang,L., Zhao,X., Feng,K., Lin,T., Lin,Z. *et al.* (2020) CRL3-SPOP ubiquitin ligase complex suppresses the growth of diffuse large B-cell lymphoma by negatively regulating the MyD88/NF-kappaB signaling. *Leukemia*, **34**, 1305–1314.
22. Goldstein,M. and Kastan,M.B. (2015) The DNA damage response: implications for tumor responses to radiation and chemotherapy. *Annu. Rev. Med.*, **66**, 129–143.
23. Liu,Y., Li,Y. and Lu,X. (2016) Regulators in the DNA damage response. *Arch. Biochem. Biophys.*, **594**, 18–25.
24. Boysen,G., Barbieri,C.E., Prandi,D., Blattner,M., Chae,S.S., Dahija,A., Nataraj,S., Huang,D., Marotz,C., Xu,L. *et al.* (2015) SPOP mutation leads to genomic instability in prostate cancer. *eLife*, **4**, e09207.
25. Hjorth-Jensen,K., Maya-Mendoza,A., Dalgaard,N., Sigurethsson,J.O., Bartek,J., Iglesias-Gato,D., Olsen,J.V. and Flores-Morales,A. (2018) SPOP promotes transcriptional expression of DNA repair and replication factors to prevent replication stress and genomic instability. *Nucleic Acids Res.*, **46**, 9484–9495.
26. Blaquiere,J.A. and Verheyen,E.M. (2017) Homeodomain-Interacting protein kinases: diverse and complex roles in development and disease. *Curr. Top. Dev. Biol.*, **123**, 73–103.
27. Hofmann,T.G., Glas,C. and Bitomsky,N. (2013) HIPK2: a tumour suppressor that controls DNA damage-induced cell fate and cytokinesis. *BioEssays*, **35**, 55–64.
28. Kuwano,Y., Nishida,K., Akaike,Y., Kurokawa,K., Nishikawa,T., Masuda,K. and Rokutan,K. (2016) Homeodomain-interacting protein kinase-2: a critical regulator of the DNA damage response and the epigenome. *Int. J. Mol. Sci.*, **17**, 10.
29. Akaike,Y., Kuwano,Y., Nishida,K., Kurokawa,K., Kajita,K., Kano,S., Masuda,K. and Rokutan,K. (2015) Homeodomain-interacting protein kinase 2 regulates DNA damage response through interacting with heterochromatin protein 1gamma. *Oncogene*, **34**, 3463–3473.
30. Liebl,M.C. and Hofmann,T.G. (2019) Cell fate regulation upon DNA damage: p53 serine 46 kinases pave the cell death road. *BioEssays*, **41**, e1900127.
31. Hofmann,T.G., Moller,A., Sirma,H., Zentgraf,H., Taya,Y., Droge,W., Will,H. and Schmitz,M.L. (2002) Regulation of p53 activity by its interaction with homeodomain-interacting protein kinase-2. *Nat. Cell Biol.*, **4**, 1–10.
32. D'Orazi,G., Cecchinelli,B., Bruno,T., Manni,I., Higashimoto,Y., Saito,S., Gostissa,M., Coen,S., Del Sal,G. *et al.* (2002) Homeodomain-interacting protein kinase-2 phosphorylates p53 at Ser 46 and mediates apoptosis. *Nat. Cell Biol.*, **4**, 11–19.
33. Singh,NP, McCoy,MT, Tice,RR and Schneider,EL. (1998) A simple technique for quantitation of low levels of DNA damage in individual cells. *Exp. Cell Res.*, **175**, 184–191.
34. S Guillamet,E, Creus,A, Farina,M, Sabbioni,E, Fortaner,S and Marcos,R. (2008) DNA-damage induction by eight metal compounds in TK6 human lymphoblastoid cells: results obtained with the alkaline Comet assay. *Mutat. Res.*, **654**, 22–28.
35. Jin,X., Wang,J., Li,Q., Zhuang,H., Yang,J., Lin,Z., Lin,T., Lv,Z., Shen,L., Yan,C. *et al.* (2019) SPOP targets oncogenic protein ZBTB3 for destruction to suppress endometrial cancer. *Am. J. Cancer Res.*, **9**, 2797–2812.
36. Winter,M., Sombroek,D., Dauth,I., Moehlenbrink,J., Scheuermann,K., Crone,J. and Hofmann,T.G. (2008) Control of HIPK2 stability by ubiquitin ligase Siah-1 and checkpoint kinases ATM and ATR. *Nat. Cell Biol.*, **10**, 812–824.
37. Calzado,M.A., de la Vega,L., Moller,A., Bowtell,D.D. and Schmitz,M.L. (2009) An inducible autoregulatory loop between HIPK2 and Siah2 at the apex of the hypoxic response. *Nat. Cell Biol.*, **11**, 85–91.
38. Imberg-Kazdan,K., Ha,S., Greenfield,A., Poultney,C.S., Bonneau,R., Logan,S.K. and Garabedian,M.J. (2013) A genome-wide RNA interference screen identifies new regulators of androgen receptor function in prostate cancer cells. *Genome Res.*, **23**, 581–591.

39. Zhang,D., Wang,H., Sun,M., Yang,J., Zhang,W., Han,S. and Xu,B. (2014) Speckle-type POZ protein, SPOP, is involved in the DNA damage response. *Carcinogenesis*, **35**, 1691–1697.
40. Dauth,I., Kruger,J. and Hofmann,T.G. (2007) Homeodomain-interacting protein kinase 2 is the ionizing radiation-activated p53 serine 46 kinase and is regulated by ATM. *Cancer Res.*, **67**, 2274–2279.
41. Bannister,A.J., Zegerman,P., Partridge,J.F., Miska,E.A., Thomas,J.O., Allshire,R.C. and Kouzarides,T. (2001) Selective recognition of methylated lysine 9 on histone H3 by the HP1 chromo domain. *Nature*, **410**, 120–124.
42. Lee,Y.H., Kuo,C.Y., Stark,J.M., Shih,H.M. and Ann,D.K. (2013) HP1 promotes tumor suppressor BRCA1 functions during the DNA damage response. *Nucleic Acids Res.*, **41**, 5784–5798.
43. Rinaldo,C., Prodosmo,A., Mancini,F., Iacovelli,S., Sacchi,A., Moretti,F. and Soddu,S. (2007) MDM2-regulated degradation of HIPK2 prevents p53Ser46 phosphorylation and DNA damage-induced apoptosis. *Mol. Cell*, **25**, 739–750.
44. Saul,V.V., de la Vega,L., Milanovic,M., Kruger,M., Braun,T., Fritz-Wolf,K., Becker,K. and Schmitz,M.L. (2013) HIPK2 kinase activity depends on cis-autophosphorylation of its activation loop. *J. Mol. Cell Biol.*, **5**, 27–38.
45. Bitomsky,N., Conrad,E., Moritz,C., Polonio-Vallon,T., Sombroek,D., Schultheiss,K., Glas,C., Greiner,V., Herbel,C., Mantovani,F. *et al.* (2013) Autophosphorylation and Pin1 binding coordinate DNA damage-induced HIPK2 activation and cell death. *PNAS*, **110**, E4203–E4212.
46. Floyd,S.R., Pacold,M.E., Huang,Q., Clarke,S.M., Lam,F.C., Cannell,I.G., Bryson,B.D., Rameseder,J., Lee,M.J., Blake,E.J. *et al.* (2013) The bromodomain protein Brd4 insulates chromatin from DNA damage signalling. *Nature*, **498**, 246–250.